*Mechanics of Composite Materials, Vol. 42, No. 2, 2006*

# BEHAVIOR OF CONCRETE CYLINDERS CONFINED BY CARBON COMPOSITE 2. PREDICTION OF STRENGTH

**V. Tamuzs,* R. Tepfers,** and E. Sparnins***

***Keywords****: confined concrete, carbon-epoxy composite, strength*

*The mechanical behavior of round concrete cylinders confined by a carbon-epoxy composite wrapping is analyzed concerning the increased concrete compression strength due the wrapping. It is shown that the loading trajectories in the normalized stress space fit into a single master curve for all the concrete batches and jacket thicknesses investigated. The loading paths ended at failure of the composite wrapping from the increased internal lateral pressure. The strength of the composite was determined by split-disc tests of composite rings, but the strength of composite jackets realized on concrete specimens did not reach the strength of the rings. Therefore, a coefficient of composite strength reduction was introduced. A simple formula for predicting the strength of confined concrete is derived, and a comparison with fib (fédération internationale du béton) recommendations for strength predictions is given.*

## 1. Introduction

A comprehensive review and an analysis of experimental results on the confinement of concrete cylinders has been given by Lorenzis and Tepfers [1], therefore, a repeated review is omitted here. A wide program [2] of experimental studies on concrete confined by a carbon-epoxy composite was carried out, the results of which are presented in [3]. A full set of experimental data is also available in [4].

Five different batches of concrete of various strength and three thicknesses of composite wrapping were used to produce specimens for tests in monotonous and repeated compressive loadings. An analysis of the experimental data obtained [3] is given in the present paper, where it is assumed that the compressive stresses and strains are positive and the tensile ones are negative.

## 1. Influence of Lateral Pressure on the Compressive Strength of Concrete.

Tests on plain concrete in triaxial compression have been reported by many authors [5-11]. In [12], results for the concrete strength $_{z}^{u}$ as a function of the lateral pressure $_{l}$ applied, normalized to the uniaxial compression strength of plain con-

*Institute of Polymer Mechanics, University of Latvia Aizkraukles St. 23, Riga, LV-1006, Latvia. **Department of Civil and Environmental Engineering, Chalmers University of Technology SE-412 96 Göteborg, Sweden. Russian translation published in Mekhanika Kompozitnykh Materialov, Vol. 42, No. 2, pp. 165-178, April-May, 2006. Original article submitted March 23, 2006.

0191-5665/06/4202-0109 

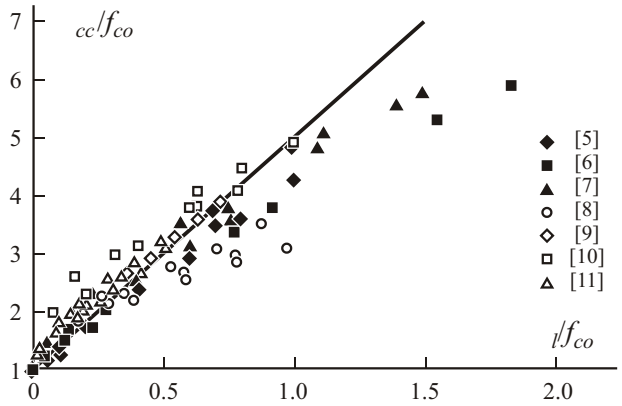


Fig. 1. Experimental data for the maximum strength $_{cc}/f_c$ vs. the lateral stress $_l/f_c$ [12]; solid line — approximation by Eq. (1) [13].

crete $f_{co}$, are summarized in one figure (Fig. 1) It is seen that all the data roughly fit into a single master curve. For a moderate lateral pressure, it is convenient to use an approximation by a straight line [13]:

$$\frac{^u_z}{f_{co}} \quad 1 \quad 4.1\frac{_l}{f_{co}} \quad \text{or} \quad ^u_z \quad f_{co} \quad 4.1 \; _l. \tag{1}$$

This line follows the well-known strength condition for brittle materials, which states that the failure occurs when the maximum strain $_{max}$ reaches its critical value

$$_{max} \quad c \quad \text{const.}$$

The lateral strain $_l$ in the elastic undamaged state is

$$_l \quad \frac{1}{E_b}[\; _l \quad (\; _l \quad _z)], \tag{2}$$

where $E_b$ is the initial Young's modulus and is the initial Poison ratio of concrete. The maximum-strain condition states that $_l \quad c$ at $_z \quad ^u_z$ for any lateral pressure, therefore

$$^u_z \quad \frac{E_b c}{} \quad \frac{_l(1 \quad )}{}.$$

In the absence of lateral pressure, we have $_{max} \quad c \quad \frac{f_{co}}{E_b}$, and it follows that

$$\frac{^u_z}{f_{co}} \quad 1 \quad \frac{(1 \quad )}{} \quad \frac{_l}{f_{co}}.$$

This equation coincides with Eq. (1) at = 0.196.

**2. Experimental Strength of Confined Concrete**

In [2-4] are given data on the compressive behavior of cylindrical concrete specimens of five different strengths and three thicknesses of the composite jacket. The tests were performed with four Teflon interlayers inserted between the end faces of the specimens and the loading platens to eliminate the friction and to better simulate the conditions in a concrete column. In this regard, these tests differ from those done by other authors. The axial and lateral deformations and the axial compression

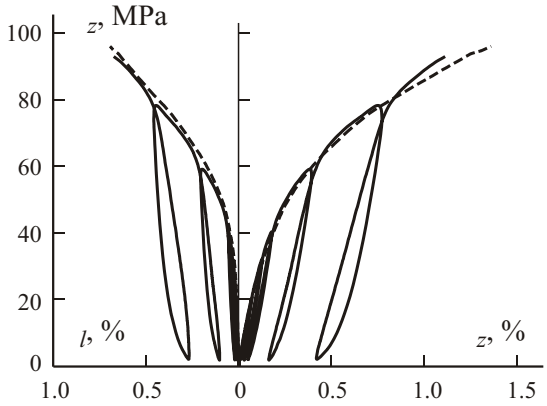


Fig. 2. Compressive behavior of the CFRP-confined concrete of batch 40 in cyclic loading (——). For comparison, the behavior of the corresponding specimen in monotonic loading is also shown (- - -).

TABLE 1. Experimental Strength Data of All the Concrete Batches Investigated

| Nominal strength, MPa | Cube strength, MPa | Cylinder strength, MPa | Cylinder strength of specimens with Teflon interlayers, MPa | Cylinder strength calculated from the cube strength, MPa |
|---|---|---|---|---|
| 20 | 34.2 | 25.2 | 20.5 | 26.6 |
| 40 | 60.5 | 47.4 | 40.7 | 43.7 |
| 60 | 76.2 | 51.8 | 44.3 | 52.6 |
| 80 | 81.4 | 70.6 | 49.7 | 55.3 |
| 100 | 104.1 | 82.1 | 61.6 | 65.7 |

load were measured during the tests. The typical stress stain–curves are displayed on Fig. 2 both for monotonous and repeated loadings.

The lateral stress $_l$ is caused by the pressure of the composite confinement and is calculated according the formula

$$_l \quad \frac{_j h}{R} \quad \frac{_l E_j h}{R}, \tag{3}$$

where $_j$ is the stress of the composite jacket, $R$ is the radius of specimens, $h$ is the thickness of the composite wrapping (only the thickness of carbon tapes, without the matrix, is taken into account), $E_j$ is Young's modulus of the carbon tape, and $_l$ is the experimental lateral strain.

The maximum lateral stress is

$$f_l \quad \frac{_j h}{R} \quad \frac{_l E_j h}{R}, \tag{4}$$

where $_j$ is the ultimate stress of the composite jacket, and $_l$ is the ultimate experimental lateral strain.

Strength values are normalized to the characteristic compressive strength of plain concrete, which depends on the specimen geometry (cubic or cylindrical) and loading conditions (the presence or absence of Teflon interlayers between speci-

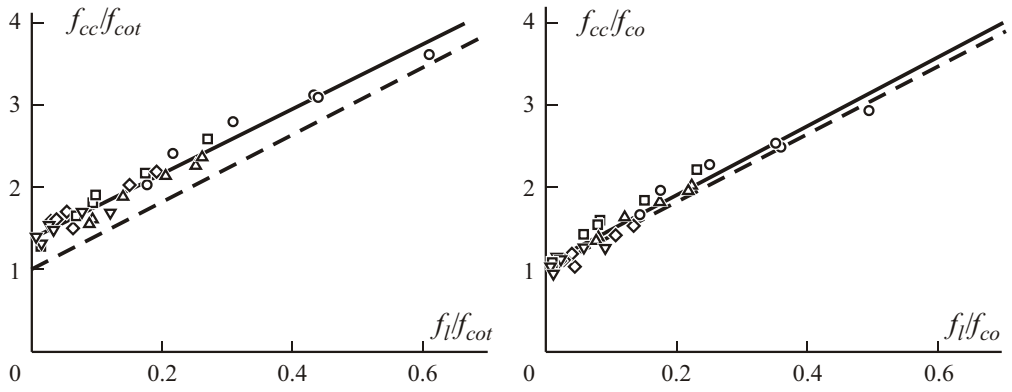


Fig. 3. Strength of concrete cylinders normalized to the strengths of plain concrete cylinder with and without Teflon interlayers, $f_{cc}/f_{cot}$ and, $f_{cc}/f_{co}$ of batches 20 (○), 40 (△), 60 (□), 80 (◇), 100 (▽). (- - -) — Eq. (1); (—) — approximation.

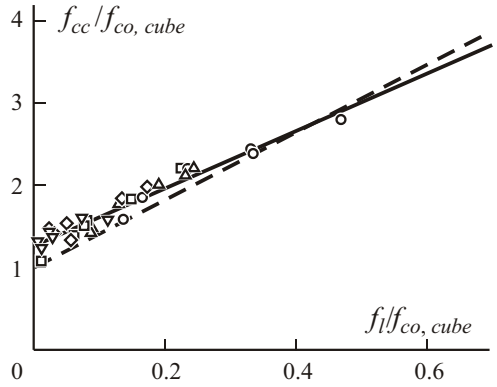


Fig. 4. Strength of concrete cylinders vs. the normalized stregth, calculated by Eq. (6). Designations as in Fig. 3.

men ends and loading plates). The strength values obtained are summarized in Table 1. All tests on the confined concrete were carried out by using Teflon interlayers, therefore, in initial calculations, the strength values for normalization were taken from identical loading conditions, namely the strengths of cylindrical specimens with Teflon interlayers, $f_{cot}$, was used, which are given in the fourth column of Table 1.

The strengths $f_{cc}$ and the corresponding lateral ultimate stresses $f_l$ for all the five batches tested and three wrapping thicknesses, normalized to the strength $f_{cot}$, are summarized in Fig. 3. The points lie along the straight line $f_{cc}/f_{cot}$ 1.38 3.94 $f_l/f_{cot}$. It is seen that the limiting normalized strength remains greater than unity when the lateral stress $f_l$ approaches zero. This means that the fracture mode of the confined concrete, even at a low confinement pressure, differs from that of plain concrete specimens with Teflon interlayers. Really, cracks in plain concrete with Teflon interlayers start at specimen ends and propagate parallel to the compression load applied. In contrary, when plain concrete without Teflon interlayers is tested, the friction at specimen ends prevents the cracking, and the damage arises somewhat later in the middle of specimens. The same effect is caused by the confinement — the lateral pressure prevents a premature failure at specimen ends, and the damage arises more evenly along the specimen length. Therefore, the strength of the confined concrete specimens should be normalized rather to $f_{co}$ than to $f_{cot}$.

On Fig.3b are shown strength data in the normalized coordinates $f_{cc}/f_{co}$ vs. $f_l/f_{co}$. The least-square deviation line for the set of experimental points is

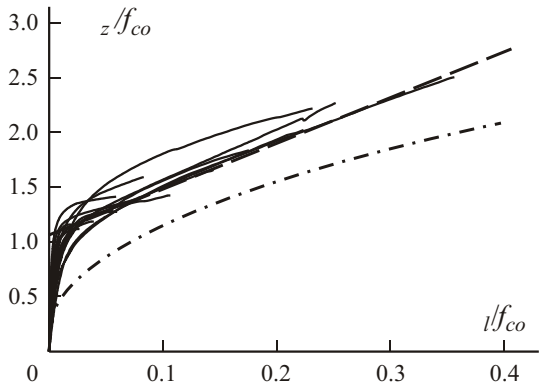


Fig. 5. Experimental loading paths for all tested samples. (- - -) — the strength of confined concrete according to Eq. (5); (-·-·-) — according to the Spoelstra–Monti formula (11).

$$\frac{f_{cc}}{f_{co}} \quad 1.06 \quad 4.20\frac{f_l}{f_{co}}. \tag{5}$$

According to the method of calculating the concrete cylinder strength from its cube strength [14],

$$f_{co,\,cube} \quad f_{cube}\,(0.85 \quad 2.1\ 10^{\ 3}\ f_{cube}). \tag{6}$$

The results are shown in the last column of Table 1. It is seen that formula (6) works fine for the concrete batches of nominal strength 20-60, but it underestimates the cylinder strength for batches 80-100. By using these values for normalizing experimental data, the graphs presented in Fig. 4 were obtained. Since the relative maximum lateral pressure of concretes 80-100 is low, the initial point of the approximation line is moved up too much, and Eq. (6) becomes

$$f_{cc}/f_{co,\,cube} \quad 1.26 \quad 3.48\,f_l/f_{co,\,cube}.$$

Therefore, in what follows, we will use formula (5), with the free term rounded to unity.

### 3. Loading Paths of Confined Concrete Specimens in Compression

The measurements of load and strain allowed us to draw loading paths in the stress space for all test specimens. On Fig. 5, the paths are displayed as $_z/f_{co}$ vs. $_l/f_{co}$. Its is remarkable that all the loading paths can be described by a single master curve.

At the initial stage of loading, the concrete is elastic. By using Eqs. (2) and (3), it can be shown that the slope of loading paths is

$$\frac{d\ _z}{d\ _l} \quad \frac{1}{k_E} \quad \frac{1}{} \quad 1,$$

where $k_E$ $\frac{E_j}{E_b}\frac{h}{R}$ is a parameter which characterizes the stiffness of confinement; $k_E$ for a completely stiff confinement, and $k_E$ 0 in the absence of confinement. The values of the parameter $k_E$ are given in Table 2 for all the specimens tested.

According to (6) and the values of $k_E$ (Table 2), the initial slope of the loading paths is about arctan (100) 89°, i.e., the loading path approaches the strength line in Fig. 5 at a rather small lateral pressure $_l/\ _{co}$ 0.001. When the loading trajec-

TABLE 2. Experimental of Values $k_E$

| Confinement | Concrete | | | | |
|---|---|---|---|---|---|
| | 20 | 40 | 60 | 80 | 100 |
| 1 layer | 0.017 | 0.012 | 0.011 | 0.012 | 0.011 |
| 2 layers | 0.040 | 0.027 | 0.027 | 0.027 | 0.026 |
| 3 layers | 0.061 | 0.042 | 0.041 | 0.042 | 0.040 |

tory reaches the strength line, the failure of concrete begins, the initial Poison ratio increases owing to the internal cracking of concrete, and the loading path becomes roughly parallel to the concrete strength line.

## 4. Strength of Composite Jacket and the Predicted Strength of Confined Concrete

The final failure of a confined specimen occurs when the composite jacket disrupts owing to the growing lateral pressure. Thus the loading paths on Fig. 5 end at the lateral pressure $_l \quad f_l$, according to Eq. (4).

Formulas (4) and (5) lead to the simple formula for the strength of confined concrete

$$\frac{f_{cc}}{f_{co}} \quad 1 \quad 4.2\frac{_j h}{f_{co} R}, \tag{7}$$

i.e., the strength of confined concrete $f_{cc}$ is predicted as

$$f_{cc} \quad f_{co}(1 \quad 4.2 \quad _s), \tag{8}$$

where the coefficient

$$_s \quad \frac{_j h}{f_{co} R}$$

characterizes the strength effectiveness of composite confinement.

For correctly predicting the strength of the confined concrete specimens, the correct value of the composite jacket strength $_j$ must be determined.

In our tests [2-4], the wrapping material was a BPE Composite 33s made from Grafil carbon fibers and epoxy resin. The data provided by the supplier are cited in Table 3.

Unfortunately, the information on the strength of fibers and its scatter (the Weibull parameters) were not available. It is well known [15] that the realization of fiber strength in a composite highly depends on the fiber volume fraction, the mean fiber strength (fixed at a certain length), and the scatter of fiber strength. Therefore, the supplier's data could not be used without correction, and the strength of the composite had to be determined in special tests. The most suitable one turned out to be the split-disk test of ring specimens according to ASTM D2290 for estimating the effective ultimate lateral strain and the ultimate stress of the composite jacket.

In Table 4, the data obtained from the split-disk test are summarized, where the reduction factor is the ratio of the experimental tensile property of CFRP to the tensile property of CFRP in uniaxial tension given by the manufacturer (Table 3). The results show that the actual tensile strength of the CFRP ring was lower with a reduction factor ranging from 0.45 to 0.60, while for the elastic modulus this factor was scattered around unity.

TABLE 3. Properties of Grafil Inc. Unidirectional 340-700 Carbon Reinforcement

| | |
|---|---|
| Tensile strength (MPa) | 4500 |
| Tensile modulus (GPa) | 234 |
| Tensile elongation (%) | 1.9 |
| Sheet thickness (mm) | 0.17 |
| Sheet width (mm) | 300 |
| Density (g/cm$^3$) | 1.8 |
| Fiber diameter ( m) | 7 |

TABLE 4. Strength Reduction Factors for CFRP Sheets

| Confinement | Strength (MPa) | Reduction factor $c_s$ | Modulus (GPa) | Reduction factor $c_E$ |
|---|---|---|---|---|
| 1 layer | 2017 | 0.45 | 189.5 | 0.81 |
| 2 layers | 2445 | 0.54 | 219.0 | 0.94 |
| 3 layers | 2670 | 0.60 | 224.9 | 0.96 |

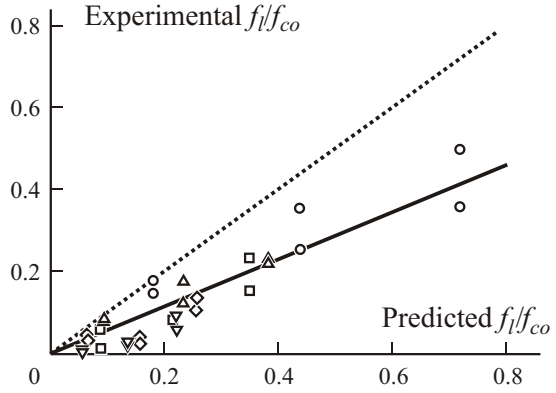


Fig. 6. Comparison between the predicted and measured values of the normalized maximum lateral stress of confined concrete. Dotted line — the ideal correspondence; solid line — the best fit; $c_b$ = 0.57. Other designations as in Fig. 3.

Unfortunately, the true strength of the composite jacket and its ultimate strain were even less than that determined in the split-disk test. A comparison between the predicted values (from Table 4 and Eq. (4)) and the measured ones for the normalized maximum lateral stress of confined concrete samples is shown on Fig. 6. A rather good correlation is seen, but the values predicted based on the split-disk test are overestimated. Therefore, to obtain the actual strength of the composite jacket, an additional reduction factor $c_b$ was introduced. The value $c_b$ = 0.57 gave the best fit with experimental data (Fig. 6, solid line).

Equation (3) now can be rewritten in the form

$$f_{cc} \quad f_{co}(1 \quad 4.2c_b \quad _s). \tag{9}$$

A comparison between the predicted and measured values of the strength of confined concrete samples is shown on Fig. 7. The line of ideal coincidence lies within the 95% confidence interval.

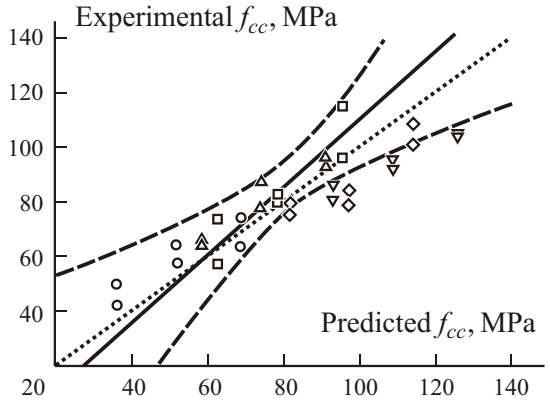


Fig. 7. Comparison between the predicted by Eq. (8) and measured values of the strength of confined concrete. (···) — the ideal correspondence; (- - -) — the 95% confidence interval; (—) — linear regression. Other designations as in Fig. 3.

**5. Comparison with the Spoelstra and Monti Formula.**

The recommendations for external strengthening and the code for design given by fédération internationale du béton [16] and the guide document by ACI [17] are based on the Spoelstra and Monti [18] approach.

The corresponding formula for predicting the strength of FRP-confined concrete has the form [16]

$$f_{cc} \quad f_{co} \quad 0.2 \quad 3\sqrt{\frac{f_l}{f_{co}}} \quad , \tag{10}$$

where $f_{cc}$ is the ultimate strength of confined concrete with Teflon layers; this strength is realized in columns; $f_{co}$ is the ultimate strength of unconfined concrete determined on standard cylinders without Teflon layers; $f_l$ is the ultimate lateral concrete strength.

Formula (10) can be interpreted in terms of the loading path in the coordinates of normalized compressive stress $_z / f_{co}$ and normalized lateral stress $_l / f_{co}$:

$$\frac{z}{f_{co}} \quad 0.2 \quad 3\sqrt{\frac{l}{f_{co}}}. \tag{11}$$

The failure occurs at $_z \quad f_{cc}$, when the stress in the composite jacket reaches the critical value $_j$ and the normalized lateral stress in concrete $_l$ reaches $f_l$. Then

$$\frac{f_l}{f_{co}} \quad \frac{_j h}{f_{co} R} \quad s,$$

and formula (10) can be rewritten in the form similar to (9)

$$f_{cc} \quad f_{co} (0.2 \quad 3\sqrt{c_b \quad s}). \tag{12}$$

Relation (10) is plotted on Fig.6 together with the experimentally determined loading paths of confined specimens and the strength line of confined concrete. It is seen that the axial stress is underestimated by Eq. (10). A comparison between the

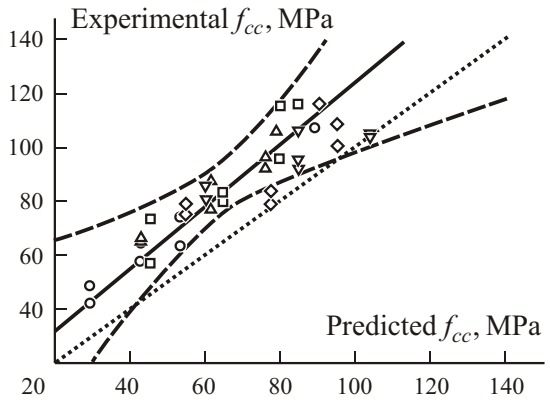


Fig. 8. Comparison between the predicted by the Spoelstra–Monti formula with reduction factor (12) and the measured values of the strength of confined concrete. (···) — the ideal correspondence; (- - -) — the 95% confidence interval; (——) — linear regression. Other designations as in Fig. 3.

predictions by Eq. (12) and the corresponding measured values for all tested specimens is shown on Fig. 8. Although Eq. (12) also underestimates the strength, it is more reliable for practical applications.

## 6. Conclusions

1) The loading paths of all the confined concrete specimens investigated fit into one master curve, which in the nonlinear region follows the strength line of plain concrete under the influence of lateral pressure.

2) The normalization of strength data for confined concrete should be done for the strength of plain concrete without Teflon interlayers.

3) For predicting the strength of confined concrete, formula (7) is recommended.

4) The experimentally measured ultimate lateral stress is significantly lower than that predicted from the fiber strength given by the manufacturer and is below the strength measured in the split-disc test. Therefore, in the formula for strength prediction, the reduction factor $c_b$ must be used.

5) The strength of confined concrete predicted by the Spoelstra–Monti formula is consistently lower than that measured experimentally.

## REFERENCES

1. L. De Lorenzis and R. Tepfers, “Comparative study of models on confinement of concrete cylinders with fiber-reinforced polymer composites,” ASCE J. Compos. Construct., 219-237 (August, 2003).
2. V. Tamuzs, Chi-Sang You, and R. Tepfers, Experimental Investigation of CFRP-Confined Concretes under Compressive Load, Institute of Polymer Mechanics, University of Latvia, Aizkraukles 23, LV-1006, Riga, Latvia and Division of Building Technology, Chalmers University of Technology, S-412 96 Goteborg, Sweden (December, 2001).
3. V. Tamuzs, R. Tepfers, Chi-Sang You, T. Rousakis, I. Repelis, V. Skruls, and U. Vilks, “Behavior of concrete cylinders confined by carbon-composite tapes and prestressed yarns. 1. Experimental data,” Mech. Compos. Mater., **41,** No. 1, 13-32 (2006).
4. http://www.pmi.lv/Assets/Files/CFRP-confined_Concrete.pdf.

5. I. Imran and S. J. Pantazopoulou, “Experimental study of plain concrete under triaxial stress,” ACI Mater. J., **93,** No. 6, 589-601 (1996).
6. D. Sfer, I. Carol, R. Gettu, and G. Etse, “Study of the behavior of concrete under triaxial compression,” J. Eng. Mech. Div. ASCE, **128**, No. 2, 156-163 (2002).
7. M. D. Kotsovos and J. B. Newman, “Generalized stress–strain relations for concrete,” J. Eng. Mech. Div. ASCE, **104**, No. 4, 845-856 (1978).
8. Q. Li and F. Ansari, “Mechanics of damage and constitutive relationships for high-strength concrete in triaxial compression,” J. Eng. Mech. Div. ASCE, **125**, No. 1, 1-10 (1999).
9. R. Bellotti and P. Rossi, “Cylinder tests: experimental technique and results,” Mater. Struct., in: RILEM 24, 45–51 (1991).
10. S. S. Smith, K. J. Willam, K. K. Gerstle, and S. Sture, “Concrete over the top, or: is there life after peak,” ACI Mater. J., **86**, No. 5, 491-497 (1989).
11. J. Xie, A. E. Elwi, and J. G. MacGregor, “Mechanical properties of three high-strength concretes containing silica fume,” ACI Mater. J., **92**, No. 2, 135–145 (1995).
12. H. Park and J.-Y. Kim, “Plasticity model using multiple failure criteria for concrete in compression,” Int. J. Solids Struct., **42**, 2303-2322 (2005).
13. M. N. Fardis and H. Khalili, “Concrete encased in fiberglass-reinforced-plastic,” J. Am. Concr. Inst. Proc., **78**, No. 6, 440-446 (1981).
14. Betonghandbok, Material (Concrete handbook, Materials; in Swedish) Editors: Ljungkrantz Ch., Muller G., Petersons N., Svensk Byggtjänst, Solna, 1994, 379-380.
15. V. P. Tamuzh, M. T. Azarova, V. M. Bondarenko, Yu. A. Gutans, Yu. G. Korabel’nikov, P. E. Pikshe, and O. F. Siluyanov, “Failure of unidirectional carbon-reinforced plastics and the realization on the strength properties of the fibers in these plastics,” Mech. Compos. Mater., **18**, No. 1, 27-34 (1982).
16. fib/CEB-FIP bulletin 14. Externally Bonded FRP Reinforcement for RC Structures. fib, Task Group 9.3 FRP Reinforcement for Concrete Structures, convenor Thanasid Triantafillou, fédération internationale du béton, Lausanne (July, 2001).
17. ACI Committee 440.2R-02, (2002). Guide for the Design and Construction of Externally Bonded FRP Systems for Strengthening Concrete Structures. American Concrete Institute, Farmington Hills, Michigan 48333-9094 (July, 2002).
18. M. R. Spoelstra and G. Monti, “FRP-confined concrete model,” ASCE J. Compos. Construct., **3**, No. 3, 143-150 (1999).